Design, Modelling, and Analysis of Legged Robot for Terrains Exploration

Ahmad O. Hourani [a], Mahmoud Z. Iskandarani [a,*]

[a] *Faculty of Engineering, Al-Ahliyya Amman University, P O Box: 19328, Amman, Jordan*
Corresponding author: [*]m.iskandarani@ammanu.edu.jo

Abstract—**Robotics design and applications become significant worldwide. In this work, an improved and upgraded Legged based robot is designed and modeled with the mathematical framework to enable rough terrain exploration. This work aims to analyze existing robots design and use it to design a better and more efficient robot that could be used in surveillance and exploration. In the proposed design, the robot's stability is the main target. The new proposed design of the robot considers such a critical parameter. In designing the optimized and improved robot, weight, cost, and the closed-loop control algorithm for this robot are closely examined, described, and analyzed with promising results. The resulting design with solar panels as a partial power supply is simulated with mathematical modeling and analysis. The special case of the robot's whole body covered with solar panels is described, characterizing curves relating drag force to solar power. The effect of safety factors and velocity is also characterized in the work. The resulting mathematical model describing curves showed a linear dependency between solar power (driving power) and drag force, with similar findings for the safety factor. However, a less linear, close-to-exponential relationship is demonstrated for velocity about the drag force. Such dynamic-legged design with supporting springs is numerically modeled using the Jacobian element, which proved to be the most suitable.**

Keywords— **Robotic design; legged structures; wheeled structures; actuators; modelling; simulation.**

I. INTRODUCTION

Researchers and industrial experts from various communities worldwide have accelerated the study and development of such a critical field due to its potential to solve problems in almost every aspect of daily life, including health, safety, education, manufacturing, military, space, and marine, among others. Mobile robots support and, in certain areas, replace people in several areas due to their capabilities. The advancement of quadruped robots is proven through deploying several successful industrial robots and the outstanding outcomes of academic research. Recently, robots have begun operating in areas that were once traditionally constrained to humans only, including homes, cooperative workplaces, and public areas. Great safety, dependability, and versatility must be attained to achieve a reliable interaction between the robot and the environment [1]. To engage with a dynamic environment, robots require a data source through data gathering and collection and a process to interpret obtained. A reliable cognitive system is required to recognize and adjust to a new environment. An accurate assessment of a robot's position and velocity is essential for reaching the goal location and cultivating a valuable picture for assessing its environment in the case of an exploration robot [2], [3]. Nowadays, robotics comprises many fields, such as robot vision, artificial intelligence, flying robots, legged robots, and wheeled mobile robots.

According to Jiang et al. [4], mobile robots' cornerstones are cognition, perception, movement, and navigation. To plan a route and execute it successfully, the robot's system must have the ability to control its traffic parameters, accurately interpret the data given by its sensors to understand any environmental variations, and continuously check its coordinates [5]. Mobile robot cognition and inference system are responsible for sensors analysis, based on which appropriate action is carried out. Thus, it runs adaptively in the robot's control system. Perception involves specialist systems like computer vision, advanced sensor technology, and signal processing. Planning algorithms and artificial intelligence must be implemented within the mobile robot system to achieve mobility and adaptive behavior. Unfortunately, mobile robots cannot perform reliable navigation in situations with complex terrains, restrictions, and environmental variety [6].

The two most known types of mobile robots are known as wheeled and legged mobile robots. Wheeled robotic movements are used extensively for the largest variety of tasks. Wheeled robots are essential for movement since they are particularly rapid and effective on paved roads. However, classic robots cannot traverse major barriers (obstacles) and uneven terrain. All-terrain robotic vehicles have difficulty navigating small obstacles and uneven terrain without expending much energy. Compared to wheeled mobile robots, legged mobile robots are known to have significantly more sophisticated locomotion techniques. In addition to not being restricted to undergoing smooth paths, one of their key benefits is that they have proven to overcome significant barriers compared to their stature [7]. According to Rathod et al. [8], overcoming solitary footholds on unsteady terrains through legged locomotion makes traveling to previously inaccessible locations possible due to wheeled robots' limitations.

As legged robots can use individual footholds, their mobility is higher over natural terrain than wheeled ones, which need a continuous support system [9]. To compensate for surface differences, legged robots can move over uneven terrain by coordinating their leg movement [10]. Legged robotic vehicles affect the terrain less than wheeled or tracked ones and require less energy to overcome entanglements. This can minimize consumed energy when traveling on smooth, soft surfaces like sand. To preserve this competent movement, legged robots can adjust their gait patterns to suit numerous terrain and obstacles [11], [12]. Moreover, the many degrees of freedom in the leg joints allow for a change of direction without slipping. Failure tolerance while engaging in static steady locomotion is another advantage of legged robots.

A wheeled robotic vehicle's ability to move is affected if one of its wheel's breaks, as it is designed to move with continuous ground support. Consequently, this proves the competence of legged robots when it comes to navigating through rough and unexpected landscapes [13]. They also have better mobility than wheeled robots, meaning they have less of an impact on the environment in which it is working. In landscapes that must mostly remain untouched or in hazardous areas, including minefields, this is extremely critical [14].

The most common application of legged robots is in remote inspection. This is due to their ability to navigate irregular terrain and unstable environments. Such robots are incredibly useful for inspecting dangerous or difficult areas for humans [15]. They have proven to have the ability to be successful in practical mobility uses by carrying out dynamic maneuvers [16]. Examples include inspecting buildings for gas leaks and assessing nuclear power plants for pollution [17].

Legged robots may move around a job site to survey the topography, take images with high-definition cameras, and produce 3D maps, providing operators with a quick and precise way to assess progress and modify designs. Legged robots can also be used in rescue missions, especially in complex and challenging terrain, and carry heavy loads for extended periods [18]. Robots with legs can navigate these surfaces and modify their gaits and maneuvers to move over obstacles and terrain.

Each four-legged animal in the natural world has developed a special ability to adapt to different situations. The motion patterns of these critters serve as inspiration for the construction of bio-inspired controls. For instance, to achieve the recurrent movement and limb synchronization of several legged robots, a neural oscillator was developed to replicate mammal gaits. Additionally, to ensure physical viability, a more flexible and reliable locomotion control was achieved by developing model-based controllers equipped with dynamic and kinematic limitations [19].

Various innovative robotic models are equipped with different numbers of legs or unique locomotion mechanisms. The tasks involved in the kinematics and dynamics of quadruped robots are analyzing and controlling the Biped robot's movements while considering the limitations imposed by its legs and joints. A combination of Cartesian and joint space coordinates is commonly utilized to describe the location and orientation of their legs.

Inverse kinematics determines the joint angles necessary to achieve a desired end-effector position. In contrast, forward kinematics involves calculating the location and orientation of the robot's end-effectors, or feet, given joint angles. Biped robots frequently need additional limitations, such as keeping the center of mass inside the support polygon, to ensure the robot's stability while moving. For biped robots to stay balanced while moving, forces and torques must be produced and controlled. This is necessary to calculate ground reaction forces and their impacts on the robot joints. Biped robots frequently use techniques like the Zero Moment Point to keep their balance when walking, which calls for the exact center of mass control and the application of the proper joint torques.

Like Biped Robots, quadruped robots use inverse and forward kinematics to describe how their legs are positioned and oriented. Calculating the forces and torques operating on the robot's legs and joints and the ground response forces during locomotion are all part of quadruped robot dynamics. This data is essential for assessing the stability and effectiveness of the robot's stride and creating control schemes for preserving balance.

A robot's leg movements to walk, trot, or run are called gaits. Evaluation of the stability, effectiveness, and viability of various leg movement patterns is a component of gait analysis. The robot's balance and stability can then be maintained using control systems such as Model Predictive Control or Central Pattern Generators. This paper aims to model and simulate an improved version of the legged robot design by looking at multiple areas of concern, including the structural design, leg actuator designs, batteries, sensors, Locomotion control and a brief on the proposed control algorithm.

II. MATERIALS AND METHOD

The main limitations of leg mobility are mechanical complexity, required power and energy consumption, visual perception, recognition, adaptive behavior to new environments, and level of intelligence. The leg, which may have many degrees of freedom, must be able to maneuver and hold the robot with a distributed robot weight over all the legs. The motor's energy efficiency is one of the most difficult problems manufacturers have to deal. Almost two-thirds of the used motor current is converted to motor heat and power dissipation in the used electronics, with the remaining one-third of the total energy converted to mechanical power.

Qi et al. [20] confirm that the complexity of legged systems' navigation and path planning would increase the required computational power. Processors have limited performance and power consumption. Therefore, for sufficient planning of a legged robot, stability between the precise route that would meet the robot's motion competence and the computational difficulty must be established [21]. Additionally, the issue of adjusting the legs in a way to support the robot safely landing on its feet needs to interact with gravity settings.

Leg coordination is a challenge in locomotion, with the correlation between gaits and the required number of robot legs [22]. The previously sought techniques for wheeled robots could be used to map and localize legged robots. However, detailed knowledge is required when working in complex and unstructured terrains [23].

Bellicoso et al. [24] worked on multi-contact force dispersion. Although a multi-limbed mobile robotic system interacts with its environment frequently, it is uncertain what contact pressures are required to support it and what are required to perform its tasks. Multi-contact movement in rough terrains especially showed a computational complication, as determining the full body path to satisfy a specific movement goal resembles a high dimensional mathematical issue that arises with a convoluted structure [25], [26]. The capacity of the legged robot to remain stable while executing its duty is one of the primary challenges faced when developing a legged robot.

The research and improvement of robotic-legged locomotion have increased during the past 20 years due to its several benefits compared to wheeled locomotion. Nevertheless, legged locomotion is still considered less reliable than other systems employing wheeled or tracked locomotion for several reasons: how much energy they consume.

The major driver of malfunctions in such robots is a result of their mechanical complication, which significantly raises the price and weight of the robot [27], [28]. The robot could lose energy due to air friction, which might also cause a problem with the stability of the robot if it is going at high speed [29], [30]. Consequently, various things need to be enhanced and optimized, given the current stage of development.

A. Structural Design

After investigating the designs of many robots and analyzing their different attributes, tools, and sensors, a new robotic structure is proposed, as depicted in Figure 1. Since the objective is to build a multi-environment robot, thus the unconventional shape shown in Figure 1 is selected, which enables better robotic stability.
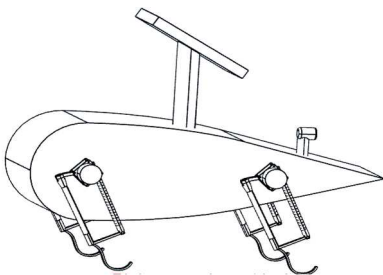

Fig. 1 Improved robotic shape

The robot would generally be expected to handle unpredictable conditions. The robot also needs a dynamic shape that limits the effects of winds and turbulent weather that could destabilize its standing and movement. In addition, the selected design is least affected by air/pressure drag, employing a wing-shaped structure for the robot's body.

The main reason for using a wing shape for the design in Figure 1 is its ability to withstand the pressure and air drags brought on by strong winds since it is built with an inclined surface curved to cut through the air and reduce drag. Figure 2 illustrates how pressure drag has a varying impact on various geometries. When air particles are compressed tightly on surfaces facing forward and spread out on surfaces facing backwards, pressure drag results. Equation (1) is used to enable shape design selection.
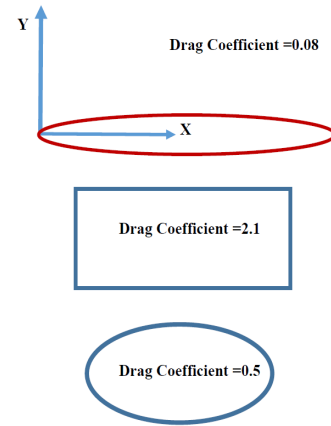

Fig. 2 Pressure/Air Drag Effects on Different Shapes

$$F_D = \left(\frac{C_D * A * \rho * V^2}{2} \right) \tag{1}$$

F_D : Drag Force
C_D : Drag Coefficient (Shape dependent)
A_f : Frontal Area
ρ : Constant density of air ($\frac{1.2\text{Kg}}{\text{m}^3}$)
V : $Robot\ Speed$

Thus, the lower the drag coefficient per shape, the less drag there is. The following C_D values for different shapes are recommended:

- Square shaped: $CD = 2.1$
- Circular shape: $CD = 1.2$
- Oval shape: $CD = 0.5$
- Wing structure: $CD = 0.08$

The wing structure possesses favorable dynamical properties from both equation (1) and the recommended coefficients. Creating electricity to recharge the robot's batteries while on a mission is essential. Thus, the design in this work includes a solar panel. One of the primary factors in using solar panels is it's lightweight. As the robot moves around, its battery will continuously be recharged, as presented in equation (2).

$$P = \left(\frac{\eta * A_s * \lambda * R}{S} \right) \tag{2}$$

P : Power required to drive the robot
η : Solar panel efficiency
A_s : Solar panel area
λ : Dust loss factor related to loss of solar efficiency
R : Solar irradiation
S : Safety factor related to atmosphere

B. Leg and Actuator Design

The actuators at each leg provide an essential thrust for the robot to jump with a stability-related design. To minimize inertia, each actuator will be placed near the shoulder of each leg, guaranteeing a safe mounting parallel to the actuator's acting springs. By concentrating the actuator mass in the hip, the parallel motion coupling reduces the inertia of the leg. Also, each actuator on each leg contributes equally during the jump's acceleration phase. To assist the robot in jumping as high as possible to escape a barrier. Segments l1 and l2, illustrated below in Figure 3, are designed to ensure that the integration of tension springs is feasible.
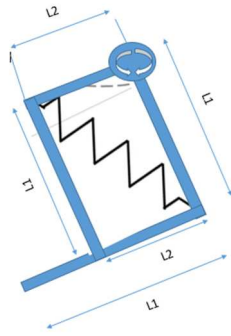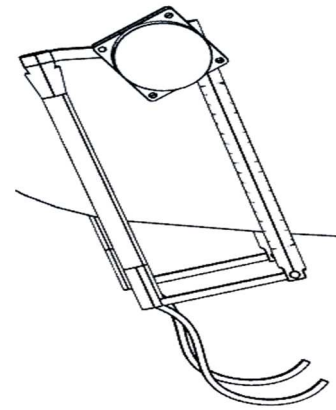

Fig. 4 Isometric leg view

Carbon tubes were chosen as the material for the links in Figure 4. Anwar et al. [31] and Rosyid et al. [32] reported that using carbon tubes as links reduced the leg's bulk and inertia. The legs also have springs built to collect and release energy during take-off and landing, significantly reducing the energy needed to perform such jumps. Electrical and hydraulic actuators are used in robots. Hydraulic actuators require a larger power-to-weight ratio than electrical ones, with heavier overall robot weight. It is suggested by Wang et al. [33] that hydraulic actuators are inappropriate for usage in certain environments like space exploration. Brushless electric DC motors are used.
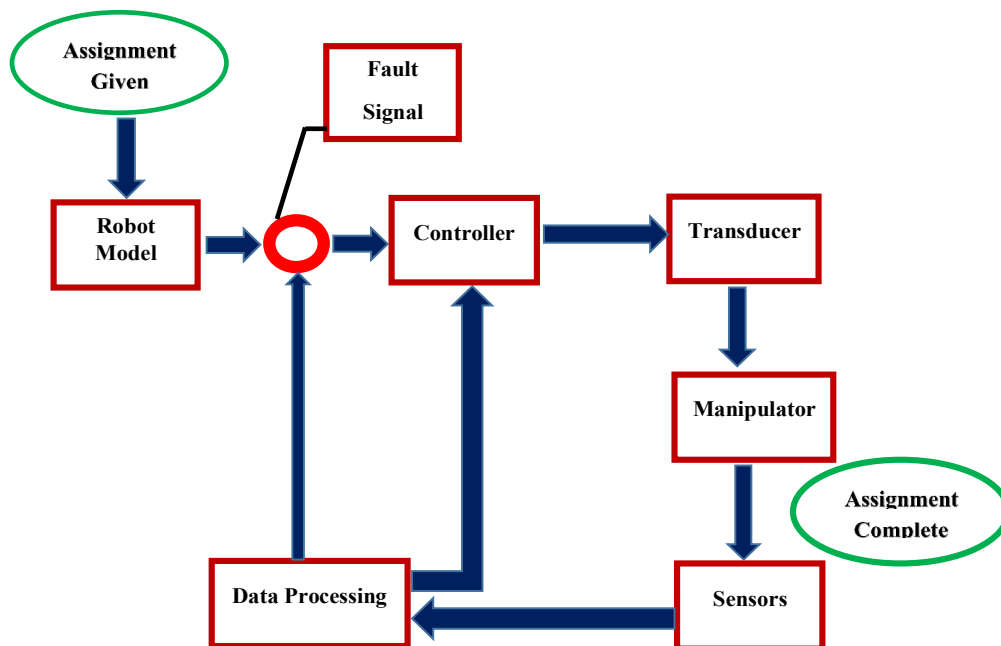

Fig. 3 Leg Kinematics

Fig. 5 Battery and Sensors

The single-stage planetary gearboxes that He et al. [34] and his group created are effective and efficient. The hip's width decreases due to the planetary gearbox inside the stator frame. The team chose a high transmission ratio of 9.55 to provide a maximum output torque of 39.5 Nm while the motor was operated at 30A. Off-axis was the "absolute magnetic rotary encoder." The ELMO Twitter Gold motor controllers drove the robot's motors inside the main body on a specially-made cooling channel. In this work, a similar actuator is employed.

A pseudo-direct method can be used to drive the robot in Figure 1, eliminating the need for force and torque sensors, as current values can be used to accurately calculate the output shaft's torque. This results in a reduction of robot weight. Even though the powertrain has a high output torque, it can be operated in reverse. Figure 5 represents the block diagram, where an already defined set task serves as the input. The definite assignment is what the robotic system produces, and the sensors keep monitoring it.

The sensors collect data and send it back as feedback signals. This is contrasted with the controller's previously assigned programmed assignment. The controller then creates the required fault signals based on the discrepancies between the given and real tasks. These are then fed back to the actuators, who use them to move the mechanical system's parts to complete the necessary work. The actuation system can handle possible high-impact loads that may be faced during landing. The motor, gearbox, aluminum frame, and bearings make up the entire drive, which is compact and lightweight (620 g per DOF).

C. Battery and Sensors

Rechargeable Li-Ion batteries are the most popular type of power storage. A robotic system can run independently for over two hours with a 650W h onboard Li-ion battery. In this work, the conventional design is enhanced by including a solar panel, which powers any LED light sensors, ultrasonic sensors, and other sensors used in the robot with the solar panel. The battery would be under less stress and could focus more on maintaining and running the engine. This can be achieved using Solar Charge Controller (SCC), which measures the current battery voltage and lowers the solar panel output voltage to a safe level. The controller reduces its output as the battery voltage approaches its threshold. One example of an SCC is the Maximum Power Point Tracking (MPPT) controller, which, by adjusting the internal resistance of the solar panel, maximizes the current output to the battery at the solar panel and modifies the load resistance.
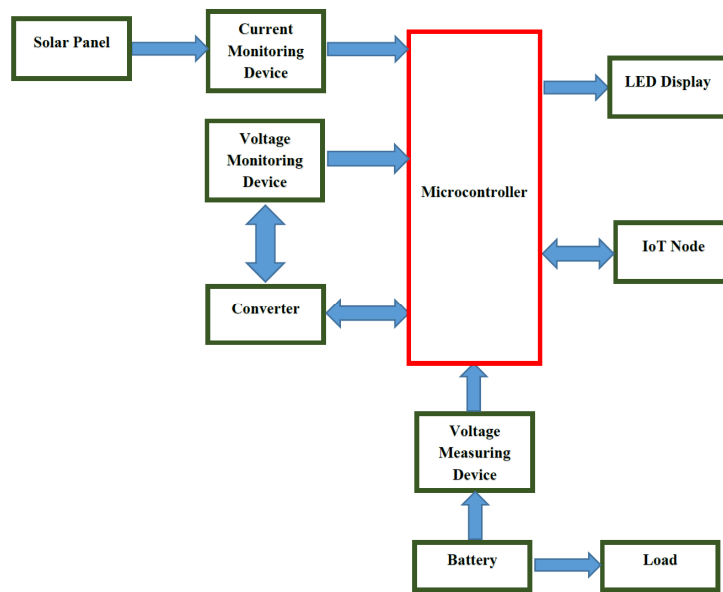

Fig. 6 Solar controller Block Diagram

Figure 6 shows a solar controller. The controller could start charging the battery with the solar panel only when the battery is empty and then stop the current flow from the solar panel to prevent charging and potential internal battery damage. A three-layer stack composed of carbon plates in Figure 7 is presented, which is lightweight. The stack will be placed at the robot's base. Carbon plates are employed to aid in safeguarding the internal components.

A legged robot system's primary sensors are the camera, Inertial Management Units (IMU), LiDARs, and tactile sensors. LiDARs have a vast range and produce incredibly accurate 3D models of the environment. They are not sensitive to the lighting or texture of the scene. However, there are disadvantages to LiDARs, including high energy consumption and a rather slow refresh rate for gathering a full scene.

Ultrasonic sensors are particularly important in robotic designs; they allow robots to detect adjacent objects. Human-like robots feature sensory systems that are similar to human senses. Initially, infrared sensors were the preferred option for this robot; however re ultrasonic sensors are unaffected by sunlight or the color of objects, unlike infrared sensors [35]. Figure 8 shows the ultrasonic transmission-reception system with a wave pattern.

Even though almost every surface reflects ultrasonic sound, it may be hard to estimate the distance to some objects, like small objects. A sonar sensor is employed in this work to support ultrasonic sensors during the exploration process to detect even small obstructions. Sonar sensing propagates acoustic energy to receive information about surroundings [36].

Researchers claim that stereo cameras could effectively help in robot navigation as both robots on wheels and legs can employ an algorithm based completely on stereo images supplied by the mounted cameras. As long as the position coordinates are provided at which the robot starts and the destination at which to arrive, the navigation system may guide the robot along a short and secure path to that destination. In terms of localization, the application utilizes visual odometry. After stereo image modeling, the terrain's topography and needed travelling path are predicted to determine the robot's best path. To accomplish this task, the d-star light algorithm is used. As shown in Figure 7, the circled area represents two stereo cameras employed for the exploration process. Compared to other 3D scanning methods, stereo cameras' features are Low-resolution, good scene illumination, and texture [37], [38].
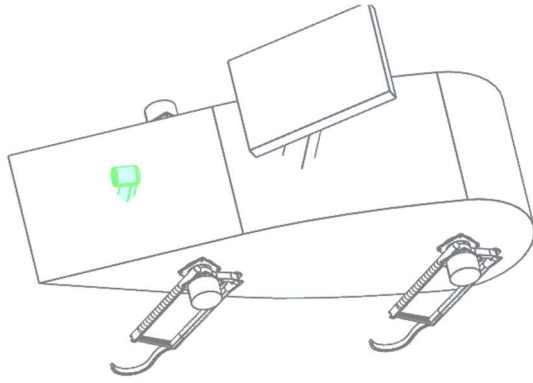
Fig. 7 Robot proposed improved design.

D. Control Architecture and Algorithm

The D-star lite algorithm is one of the effective algorithms for controlling the robot. By taking terrain mapping into account, along with additional features like path discovery, the algorithm can discover the shortest and most appropriate path for the designed robot, thus enabling the moving robot to explore the surroundings efficiently. D-star Lite plans the path between the starting point and the final destination. This distinction is useful for bidirectional planning because travelling backward involves fewer alterations when a path needs to be generated.

The D-star light algorithm is based on using nodes connected by edges. Two scores are assigned to each node in a given graph (cost to the parent of the node and the cost to the node itself), and D-star Lite keeps track of them. The right-hand side (RHS) score can provide a more accurate estimate. The system uses this score to determine the pathfinder's next optimum position computing one step ahead and comparing cost. Using these two scores, the technique creates a path from the destination to the starting point, eventually identifying the most efficient path [39].

E. Locomotion and Control

A mobile robot should possess locomotion technology to enable its free movements. There are many ways a robot can move; thus, selecting a locomotion strategy is critical for mobile robot design. The effectiveness of legged movement is dictated by the leg mass and body mass, which the robot must sustain at different moments throughout a legged stride.

The key advantages are maneuverability and agility in rough terrain, where every leg has two degrees of freedom. Controlling the gait or coordinating the leg's movements is challenging for a mobile robot with multiple legs. The gait consists of each leg's lift and release movements. The overall number of possible outcomes for a walking robot is shown in equation (3) [40]. This work uses 5,040 gaits as computed using equation (3).

$$N = (2k - 1)! \qquad (3)$$

Where;
N: Total number of outcomes
K: Number of robot legs

The locomotion controller allows the robot to choose from various gaits as a function of the environment. This work's proposed designed robot will depend on a Virtual Model Controller (VMC). Using a VMC, which mimics virtual actuators by using joint actuators, will assist in resolving the control issue. The VMC uses a Jacobian matrix to determine the joint and control torques.

There are two main gaits used in this work:

1) Leaping Gait: Two control strategies are used, depending on whether the robot is in close touch with the ground. When the robot is in the jumping phase, the foot controller for its position will be in operation. When a VMC is used, the controller selects the necessary virtual torques and forces them to be applied to the robot's center of gravity.

The controller uses the velocity error to calculate the virtual force in the x direction, f_x. Calculating the force in the z-direction, or f_z, that causes the gait to jump requires using a virtual spring model. To account for this, the respective spring constant, k_{p-z-f}, is larger during the acceleration phase than during the deceleration phase. The virtual torque is given using equations (4) and (5).

$$f_x = k_{p-x-f}(v^*_x - v_x) \qquad (3)$$
$$f_x = k_{p-z-f}(r^*_z - r_z) + mg \qquad (5)$$

Where mg represents the gravitational force, and v represents the velocity.

2) Walking Gaits

The VMC will carry out walking gaits, including a walking trot, a static walk, and a dynamic diagonal walk. The stance phase of gait begins when the foot first contacts the ground and emerges from the ground. The swing phase of the gait is defined as beginning as soon as the foot leaves the ground and ending when the foot makes contact with the ground. The controller for the walking gait is depicted in Figure 8.

The desired torso motion is achieved using leg motions. The torso is kept in the desired position throughout the walking pattern. The motion of the torso along the x-axis is calculated using the total of the foot positions considering leg weights. Depending on whether the leg is on the ground or not, the weight changes.
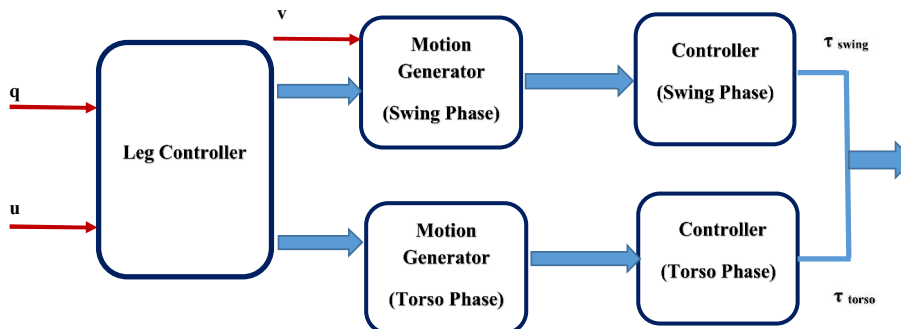

Fig. 8 Walking Gait Controller

The required position and velocity are tracked in both the horizontal and vertical directions using the same VMC that is used to track the motion of the torso. Limitations provide the desired minimal normal forces to maintain contact between the stance feet and the ground and limit tangential forces to prevent the feet from slipping. Foot forces are translated into motor torques using Jacobian transposition mapping. Another option is to use the footpath controller because the VMC method's gaits cannot be used to spin the legs. After all, slippage is required and is prevented by the previously noted constraint. Foot courses, however, are designed for a running stride.

The design and simulation employed the following parameters:

- A safety factor of 1.5.
- Robot operational power is around 100W.
- Solar panel efficiency is around 27.5%, with a dust loss factor of 0.7.

A solar panel area of approximately 1.325m^2 would result from plugging the variables into equation (2). The design of a mobile robot requires careful consideration of its locomotion strategy. Legged locomotion provides maneuverability and agility in rough terrain, with each leg having two degrees of freedom. This makes it particularly suitable for navigating challenging environments that wheeled or tracked robots may find difficult to traverse. The gait system, consisting of a sequence of lift and release movements for each leg, enables the robot to adapt to various terrains by adjusting its walking pattern. Utilizing a Virtual Model Controller (VMC) simplifies the control challenge by mimicking virtual actuators and using a Jacobian matrix to determine joint and control torques.

The proposed design includes leaping and walking gaits. The leaping gait is controlled using virtual forces and torques, allowing the robot to jump and navigate obstacles effectively. The walking gaits, such as a walking trot, static walk, and dynamic diagonal walk, utilize the VMC to maintain the desired torso position and provide stability during the robot's motion. These gaits enable the robot to move efficiently and adapt to different terrain conditions.

Additionally, the footpath controller offers an alternative to the VMC method, allowing for more flexibility in leg movement during running strides. This further enhances the robot's adaptability and maneuverability in diverse environments. This gait system should be used because it offers a versatile and adaptive locomotion strategy for a mobile robot, enabling it to effectively navigate complex terrains and overcome obstacles with greater ease than traditional wheeled or tracked systems.

III. RESULTS AND DISCUSSION

To model, assemble, render, and animate the proposed improved design of the legged robot, Solidworks was utilized. Restraints were put in place to fix the body, shell, cameras, and solar panel using the fixture button depicted in Figure 9.
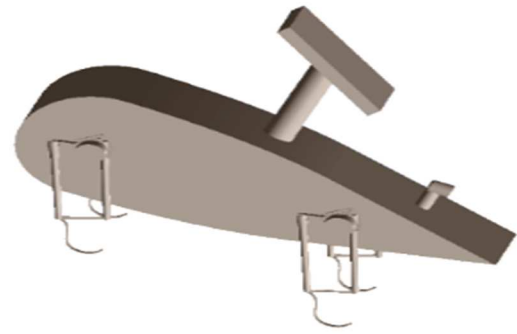

Fig. 9 Parts setting

Depending on the part, it can be fixed independently or via the links that connect it to another section of the robot. Furthermore, a 2kN external load is applied. This is demonstrated in Figures 10 and 11. Figure 10 depicts the expected direction of the load, and Figure 11 displays the meshing of the built-in model with the limitations applied.
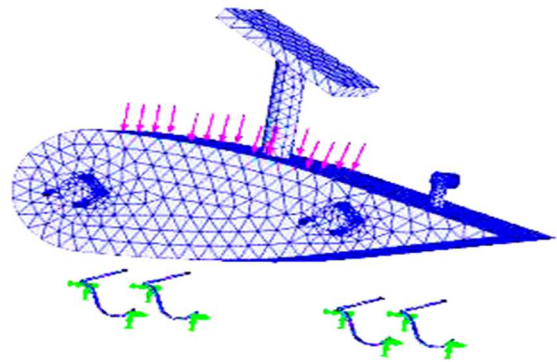
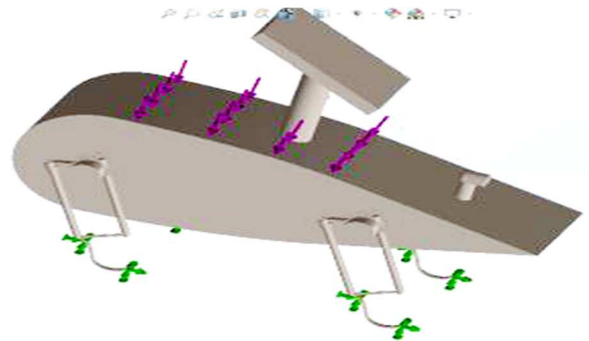

Fig. 10 External load setting

Fig. 11 Model meshing

Solidworks is used to analyze the aspect ratio after examining the external loads. The aspect ratio serves as a gauge of the elements' quality. According to its definition, it is "the ratio between the longest edge and the shortest normal dropped from a vertex to the opposite face, normalized concerning a perfect tetrahedral." Furthermore, a perfect tetrahedral element has an aspect ratio of one by nature. According to the aspect ratio check, the four corner nodes are supposed to be connected by straight edges. The software determines the aspect ratio to assess the mesh quality. Given that, a mesh of decent quality would have an aspect ratio less than the outcome is depicted in Figure 12.

The Jacobian Ratio measures the deviation between an element's actual and ideal shape. The perfect ratio is one. The software calculates every element's Jacobian ratio at the

predetermined number of Gaussian points. The stochastic study suggests that a Jacobian ratio of under 30 is appropriate. The software automatically adjusts the positions of the distorted components' central nodes to ensure that all deformed elements pass the Jacobian ratio test. The Jacobian ratio is the ratio of the highest to minimum determinant value. Figure 13 displays the results and the minimum and maximum value yields. The Jacobian ratio check is built upon several points within each element. At, Jacobian ratios are evaluated.
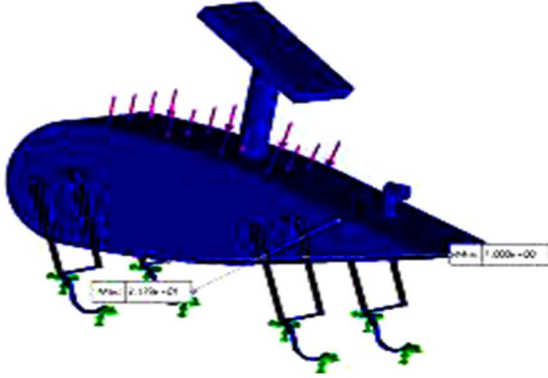

Fig. 12 Design with an aspect ratio

However, the results obtained by applying a force load and a regulated displacement load differ to some extent but are generally the same. The mismatch is due to the force-loaded face in the model not staying flat. This face experiences displacement overall, although it does not change in the necessary displacement model.
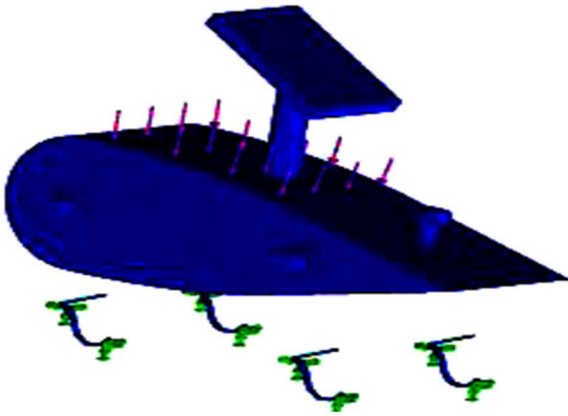

Fig. 13 Simulation with Jacobian

From equations (1) and (2), assuming that the whole robot area is covered with solar panels, then both equations can be re-arranged in terms of area results in equations (6) and (7)

$$A = \left(\frac{2F_D}{C_D * \rho * V^2}\right) \qquad (6)$$

$$A_s = \left(\frac{S*P}{\eta * \lambda * R}\right) \qquad (7)$$

Equations (6) and (7) can be rewritten as in equations (8) and (9).

$$A = \left(\frac{2F_D}{\Phi}\right) \qquad (8)$$

$$A_s = \left(\frac{S*P}{\Psi}\right) \qquad (9)$$

Thus, dragging force, F_D can be computed about solar power with safety coefficient, assuming that the robot's body area is fully covered with wearable solar panels. Thus, it is assumed that $A = A_s$. This relationship is shown in equation (10).

$$F_D = (S * P)\left(\frac{\Phi}{2\Psi}\right) \qquad (10)$$

From equation (10), three cases can be introduced:

1) Effect of solar power: The power to operate the robot is altered over the range of (75-120) W with a 5 W difference for every, with $\left(\frac{\Phi}{2\Psi}\right)$ fixed as a constant ratio, selected based on experimental values. Thus, $(0.001327 Nm^{-3}s^{-2}kg)$, and the safety factor of 1.5 will be used. The resulting curve is shown in Figure 14.
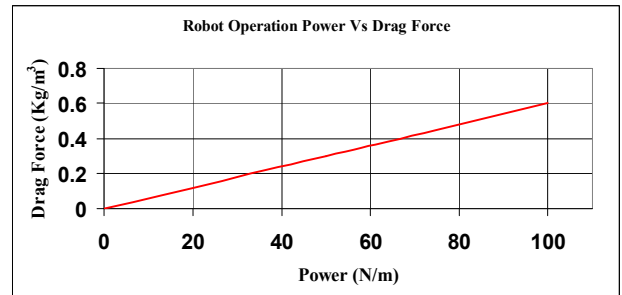

Fig. 14 Driving power and drag Force relationship

2) Effect of safety factor: Using $100W$ as the power to drive the robot during its mission, along with the same ratio of $\left(\frac{\Phi}{2\Psi}\right)$ from equation (10). The relationship between the safety factor and the drag force is shown in Figure 15.
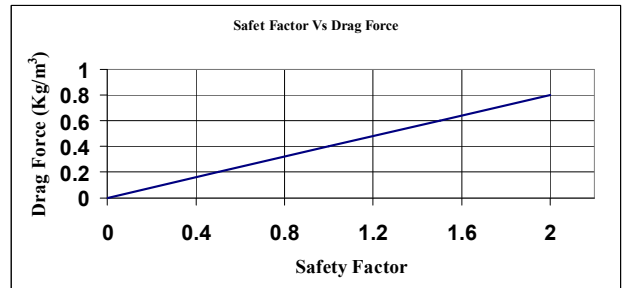

Fig. 15 Safety factor and drag force Relationship.

3) Effect of robot velocity: By fixing all variables and varying the velocity of the robot within the term $\left(\frac{\Phi}{2\Psi}\right)$ And by keeping the robot's driving power and the safety factor constant at 100 W and 1.5, respectively, Figure 16 is obtained.
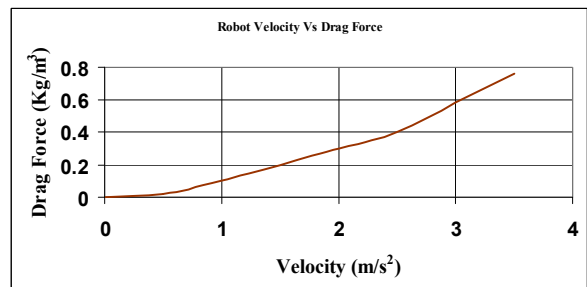

Fig. 16 Effect of robot velocity on drag force

1134

The results in Figures 14 to 16 show a predominantly linear relationship prescribing drag force, with less linearity under the influence of velocity. Such characterization is also a result of the optimized design.

IV. Conclusion

In this work, an improved legged robot model is designed, modelled, and simulated. With an improved locomotion system, the proposed design could be built with the necessary sensors and controls to enable smoother robotic movements under different scenarios. The required sensors and their interfaces (pressure, accelerometers, and strain gauges), which can be used to calculate slip and employed in contact detection, could be handled by a Spartan 3A FPGA. Additionally, Time of Flight (TOF) cameras, which provide high-speed imagery with the ability to capture an entire scene, can be utilized in place of the stereo cameras employed by my robot. This enables economically viable prototype production.

The use of solar panels in the proposed model is one of the key features to enable mobility and reduce reliance on robot charging. The employed solar panel was used to power the sensors, cameras, and any LED light sensors, giving the battery additional time to run. Power generation is intermittent since it depends on the solar cycle but also on environmental conditions like dust buildup and shading. The developed mathematical model and characterization curves also support such an optimum design.

Future work should investigate the viability of building a robot that can walk and fly using turbines for future relevant research in this subject. This should result in a novel locomotion style, where the robot would effortlessly fly over any met obstacles to transcend them and continue carrying out its work, even if more power would be required to achieve it.

References

[1] A. Torres-Pardo et al., "Legged locomotion over irregular terrains: state of the art of human and robot performance," Bioinspiration and Biomimetics, vol. 17, no. 6, 2022, doi: 10.1088/1748-3190/ac92b3.

[2] D. Wisth, M. Camurri, and M. Fallon, "VILENS: Visual, Inertial, Lidar, and Leg Odometry for All-Terrain Legged Robots," IEEE Trans. Robot., vol. 39, no. 1, pp. 309–326, 2023, doi: 10.1109/TRO.2022.3193788.

[3] M. Merschformann, T. Lamballais, M. B. M. de Koster, and L. Suhl, "Decision rules for robotic mobile fulfillment systems," Oper. Res. Perspect., vol. 6, no. October, p. 100128, 2019, doi: 10.1016/j.orp.2019.100128.

[4] R. Jiang, B. He, Z. Wang, Y. Zhou, S. Xu, and X. Li, "A Novel Simulation-Reality Closed-Loop Learning Framework for Autonomous Robot Skill Learning," IEEE Trans. Cogn. Dev. Syst., vol. 14, no. 4, pp. 1520–1531, 2022, doi: 10.1109/TCDS.2021.3118294.

[5] F. Rubio, F. Valero, and C. Llopis-Albert, "A review of mobile robots: Concepts, methods, theoretical framework, and applications," Int. J. Adv. Robot. Syst., vol. 16, no. 2, pp. 1–22, 2019, doi: 10.1177/1729881419839596.

[6] J. Wang et al., "A survey of learning-based robot motion planning," IET Cyber-systems Robot., vol. 3, no. 4, pp. 302–314, 2021, doi: 10.1049/csy2.12020.

[7] D. D. Fan, A. A. Agha-Mohammadi, and E. A. Theodorou, "Learning Risk-Aware Costmaps for Traversability in Challenging Environments," IEEE Robot. Autom. Lett., vol. 7, no. 1, pp. 279–286, 2022, doi: 10.1109/LRA.2021.3125047.

[8] N. Rathod et al., "Model Predictive Control with Environment Adaptation for Legged Locomotion," IEEE Access, vol. 9, pp. 145710–145727, 2021, doi: 10.1109/ACCESS.2021.3118957.

[9] T. Mikolajczyk et al., "Drive , Sensors and Control Systems," Sensors (Switzerland), pp. 1–31, 2022.

[10] B. Chong et al., "A general locomotion control framework for multi-legged locomotors," Bioinspiration and Biomimetics, vol. 17, no. 4, 2022, doi: 10.1088/1748-3190/ac6e1b.

[11] D. Drotman, S. Jadhav, D. Sharp, C. Chan, and M. T. Tolley, "Electronics-free pneumatic circuits for controlling soft-legged robots," Sci. Robot., vol. 6, no. 51, 2021, doi: 10.1126/SCIROBOTICS.AAY2627.

[12] M. Luneckas et al., "Hexapod robot gait switching for energy consumption and cost of transport management using heuristic algorithms," Appl. Sci., vol. 11, no. 3, pp. 1–13, 2021, doi: 10.3390/app11031339.

[13] G. Picardi, H. Hauser, C. Laschi, and M. Calisti, "Morphologically induced stability on an underwater legged robot with a deformable body," Int. J. Rob. Res., vol. 40, no. 1, pp. 435–448, 2021, doi: 10.1177/0278364919840426.

[14] C. Prados, M. Hernando, E. Gambao, and A. Brunete, "MoCLORA—An Architecture for Legged-and-Climbing Modular Bio-Inspired Robotic Organism," Biomimetics, vol. 8, no. 1, p. 11, 2022, doi: 10.3390/biomimetics8010011.

[15] G. Xin et al., "Variable Autonomy of Whole-body Control for Inspection and Intervention in Industrial Environments using Legged Robots," IEEE Int. Conf. Autom. Sci. Eng., vol. 2020-Augus, pp. 1415–1420, 2020, doi: 10.1109/CASE48305.2020.9216813.

[16] C. Zhao and W. Guo, "Inverted Modelling: An Effective Way to Support Motion Planning of Legged Mobile Robots," Chinese J. Mech. Eng. (English Ed., vol. 36, no. 1, 2023, doi: 10.1186/s10033-023-00851-3.

[17] A. Dettmann, D. Kühn, and F. Kirchner, "Control of active multi-point-contact feet for quadrupedal locomotion," Int. J. Mech. Eng. Robot. Res., vol. 9, no. 4, pp. 481–488, 2020, doi: 10.18178/ijmerr.9.4.481-488.

[18] M. Rafeeq, S. F. Toha, S. Ahmad, M. S. M. Yusof, M. A. M. Razib, and M. I. H. S. Bahrin, "Design and Modeling of Klann Mechanism-Based Paired Four Legged Amphibious Robot," IEEE Access, vol. 9, pp. 166436–166445, 2021, doi: 10.1109/ACCESS.2021.3135706.

[19] S. Fahmi, C. Mastalli, M. Focchi, and C. Semini, "Passive Whole-Body Control for Quadruped Robots: Experimental Validation over Challenging Terrain," IEEE Robot. Autom. Lett., vol. 4, no. 3, pp. 2553–2560, 2019, doi: 10.1109/LRA.2019.2908502.

[20] J. Qi, H. Gao, H. Yu, M. Huo, W. Feng, and Z. Deng, "Integrated attitude and landing control for quadruped robots in asteroid landing mission scenarios using reinforcement learning," Acta Astronaut., vol. 204, no. March, pp. 599–610, 2023, doi: 10.1016/j.actaastro.2022.11.028.

[21] J. He and F. Gao, "Mechanism, Actuation, Perception, and Control of Highly Dynamic Multilegged Robots: A Review," Chinese J. Mech. Eng. (English Ed., vol. 33, no. 1, 2020, doi: 10.1186/s10033-020-00485-9.

[22] L. Mao, F. Gao, Y. Tian, and Y. Zhao, "Novel method for preventing shin-collisions in six-legged robots by utilising a robot–terrain interference model," Mech. Mach. Theory, vol. 151, 2020, doi: 10.1016/j.mechmachtheory.2020.103897.

[23] I. Torroba, C. I. Sprague, and J. Folkesson, "Fully-Probabilistic Terrain Modelling and Localization with Stochastic Variational Gaussian Process Maps," IEEE Robot. Autom. Lett., vol. 7, no. 4, pp. 8729–8736, 2022, doi: 10.1109/LRA.2022.3182807.

[24] C. D. Bellicoso et al., "Advances in real-world applications for legged robots," J. F. Robot., vol. 35, no. 8, pp. 1311–1326, 2018, doi: 10.1002/rob.21839.

[25] C. Boussema, M. J. Powell, G. Bledt, A. J. Ijspeert, P. M. Wensing, and S. Kim, "Online gait transitions and disturbance recovery for legged robots via the feasible impulse set," IEEE Robot. Autom. Lett., vol. 4, no. 2, pp. 1611–1618, 2019, doi: 10.1109/LRA.2019.2896723.

[26] Ç. Kaymak, A. Uçar, and C. Güzeliş, "Development of a New Robust Stable Walking Algorithm for a Humanoid Robot Using Deep Reinforcement Learning with Multi-Sensor Data Fusion," Electron., vol. 12, no. 3, 2023, doi: 10.3390/electronics12030568.

[27] A. Bratta, M. Focchi, N. Rathod, and C. Semini, "Optimization-Based Reference Generator for Nonlinear Model Predictive Control of Legged Robots," *Robotics*, vol. 12, no. 1, pp. 1–18, 2023, doi: 10.3390/robotics12010006.

[28] Y. Tang, G. Zhang, D. Ge, C. Ren, and S. Ma, "Undulatory gait planning method of multi-legged robot with passive-spine," *Biomim. Intell. Robot.*, vol. 2, no. 1, p. 100028, 2022, doi: 10.1016/j.birob.2021.100028.

[29] H. Ou, H. Yi, Z. Qaiser, T. Ur Rehman, and S. Johnson, "A Structural Optimization Framework to Design Compliant Constant Force Mechanisms With Large Energy Storage," *J. Mech. Robot.*, vol. 15, no. 2, pp. 1–10, 2023, doi: 10.1115/1.4054766.

[30] W. Wu, L. Gao, and X. Zhang, "A Stability Training Method of Legged Robots Based on Training Platforms and Reinforcement Learning with Its Simulation and Experiment," *Micromachines*, vol. 13, no. 9, 2022, doi: 10.3390/mi13091436.

[31] S. F. Z. Anwar, Y. Wang, W. Raza, G. Arnold, and W. Wang, "Mechanical energy fluctuation in lower limbs during walking in participants with and without total hip replacement," *R. Soc. Open Sci.*, vol. 10, no. 3, 2023, doi: 10.1098/rsos.230041.

[32] A. Rosyid, C. Stefanini, and B. El-Khasawneh, "A Novel Walking Parallel Robot for On-Structure Three-Axis Machining of Large Structures," *J. Mech. Robot.*, vol. 15, no. 6, pp. 1–10, 2023, doi: 10.1115/1.4056682.

[33] L. Wang *et al.*, "Design and implementation of symmetric legged robot for highly dynamic jumping and impact mitigation," *Sensors*, vol. 21, no. 20, pp. 1–16, 2021, doi: 10.3390/s21206885.

[34] J. He, Y. Sun, L. Yang, and F. Gao, "Model Predictive Control of a Novel Wheeled–Legged Planetary Rover for Trajectory Tracking," *Sensors*, vol. 22, no. 11, 2022, doi: 10.3390/s22114164.

[35] T. Kelemenová and E. Jakubkovič, "Condition of Ultrasonic Distance Measurement System," *Acta Mechatronica*, vol. 4, no. 2, pp. 1–5, 2019, doi: 10.22306/am.v4i2.47.

[36] W. Jansen, D. Laurijssen, and J. Steckel, "Real-Time Sonar Fusion for Layered Navigation Controller†," *Sensors*, vol. 22, no. 9, pp. 1–20, 2022, doi: 10.3390/s22093109.

[37] Y. Alkendi, L. Seneviratne, and Y. Zweiri, "State of the Art in Vision-Based Localization Techniques for Autonomous Navigation Systems," *IEEE Access*, vol. 9, pp. 76847–76874, 2021, doi: 10.1109/ACCESS.2021.3082778.

[38] G. Haddeler *et al.*, "Traversability analysis with vision and terrain probing for safe legged robot navigation," *Front. Robot. AI*, vol. 9, no. August, pp. 1–14, 2022, doi: 10.3389/frobt.2022.887910.

[39] H. Huang, Y. Li, and Q. Bai, "An improved A star algorithm for wheeled robots path planning with jump points search and pruning method," *Complex Eng. Syst.*, vol. 2, no. 3, p. 11, 2022, doi: 10.20517/ces.2022.12.

[40] A. N. A. Rafai, N. Adzhar, and N. I. Jaini, "A Review on Path Planning and Obstacle Avoidance Algorithms for Autonomous Mobile Robots," *J. Robot.*, vol. 2022, 2022, doi: 10.1155/2022/2538220.